ALIGNMENT OF TARN II

Akira Noda*, Morio Yoshizawa, Tamaki Watanabe, Toshiaki Osuka* *,
Takeshi Katayama, Akird Mizobuchi
Institute for Nuclear Study, University of Tokyo, Midori-cho 3-2-1, Tanashi-city, Tokyo 188, Japan

Kazushi Emoto
Nihon Kensetsu Kogyo, Co., Ltd., ShinbashiS-13-11, Minato-ku, Tokyo 105, Japan

1. Introduction

TARN II is a heavy ion synchrotron/cooler ring, whose average radius and circumference are 12.4 m and 77.8 m, respectively. Main parameters of TARN II are listed up in Table 1[1]. As the radius of curvature of dipole is 4.045 m and the deflection angle of each dipole magnet is I5°, the method to set the magnets on the equilateral triangles around the ring center is considered to be more effective compared with such a method as "perpendicular-short chord" or "short-long chord" measurement[2]. The ring is set in the experimental hall composed of three parts between which two walls exist as shown in Fig. 1. So some distances of the magnets from the center cannot be measured. In order to keep the hexagonal shape of TARN II ring, special care is needed and algorithm to calculate the optimum position correction to each magnet based on Householder's method has been developed.
Positioning holes whose positions are precisely controlled at the fabrication stage of the magnet are made on each magnet. The distances between the positioning holes on the magnets and center pole are measured by a distometer utilizing Invar wires 1.0 mm in diameter (made by Kern Co. Ltd.). The absolute value of the distance is calibrated on a straight rail with use of a laser interferometer (HP 5526A) at each measurement. The distometer measures the difference of the distance to be measured from the known distance on the calibration rails.

In the present paper, the algorithm of the positioning of the magnets are given, then real alignment procedure is described together with the final results of alignment of TARN II.

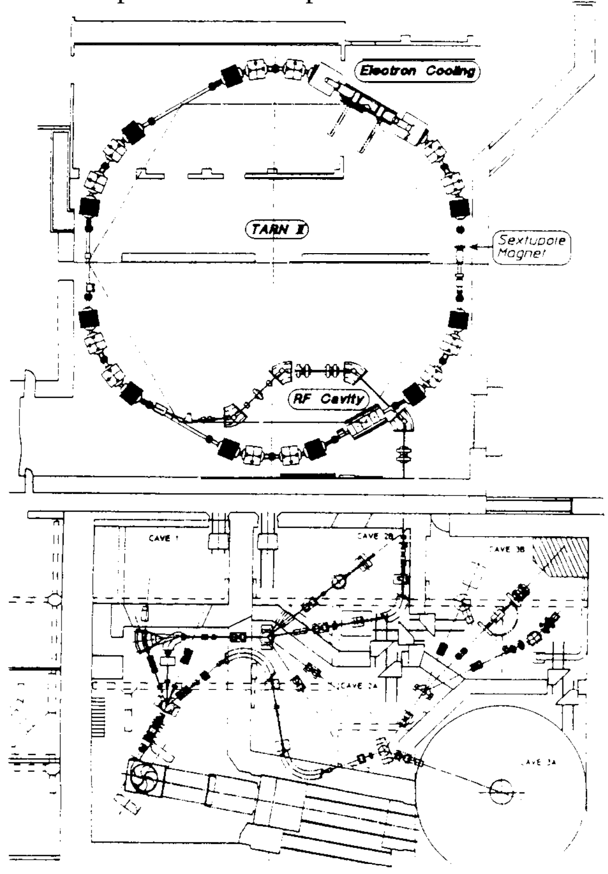

Fig. 1 Layout of TARN II.

*Present address: Institute for Chemical Research, Kyoto University

**Present address: College of Arts and Sciences, Chiba University

2. Algorithm of the Alignment

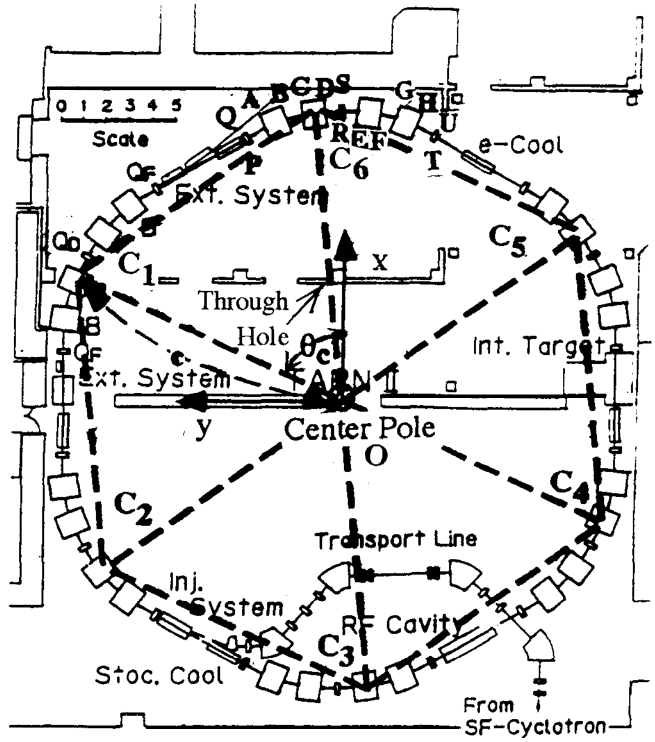

Fig. 2 Distances to be measured to keep regular hexagonal shape.

The TARN II ring should be positioned on a regular hexagon as shown in Fig. 1, because it has superperiodicity of 6. As the ring is set in a experimental hall not in an accelerator tunnel, it is decided to be aligned relative to the center pole. The problem to be solved here is due to the fact that there exist two walls almost the middle of the experimental hall as shown in Fig.1. The main magnet system is composed of 24 dipole and 18 quadrupole magnets(12 Q_F and 6 Q_D). These magnets are divided into 7 subgroups (4 subgroups of dipoles and three ones of quadrupoles). Any member in each subgroup is overlapped with the other member of the same subgroup by such a rotation around the center pole as large as integral multiple of 60°. As each magnet has three degrees of freedom, each subgroup has 18 unknowns and the same or larger number of constraints are needed to solve these unknowns. In order to keep regular hexagonal shape for the whole ring, it is needed that at least one subgroup should be positioned on the regular hexagonal shape by measuring distances between the center pole and the member magnets together with the sides between these magnets as shown in Fig. 2. For this purpose, we have made a through hole on one of the walls to enable the needed distance measurements as is indicated in Fig.2. Once a subgroup is well positioned, the regular hexagonal shape is kept also for the other subgroup with the constraints of the distances from the magnets in the subgroup which is already positioned as shown in Fig. 3, even if some distances of the magnets from the center pole cannot be measured due to the presence of the walls. The algorithm to position magnets in each subgroup is presented below.

Table 1
Main Parameters of TARN II

Maximum Energy	Proton	1300 (MeV)
	Ions with ε =1/2	450 (MeV/u)
Circumference		77.761 (m)
Average Radius		12.376 (m)
Radius of Curvature		4.045 (m)
Focusing Structure		FBDBFO
Superperiodicity		6
		(3 for Cooler Ring Mode)
Betatron Tune		1.75
Dipole Magnet		
Number		24
Deflection Angle		15°
Quadrupole Magnet		
Number		18
Core Length		0.2 (m)

2.1. Algorithm of Position Feed-back with use of Measured Distances

The distances necessary to keep regular hexagonal shape can be measured by making through holes in the wall as shown in Fig. 2 for the subgroup of magnets having positioning holes named C and D_i (i=1~6). Let's assume the

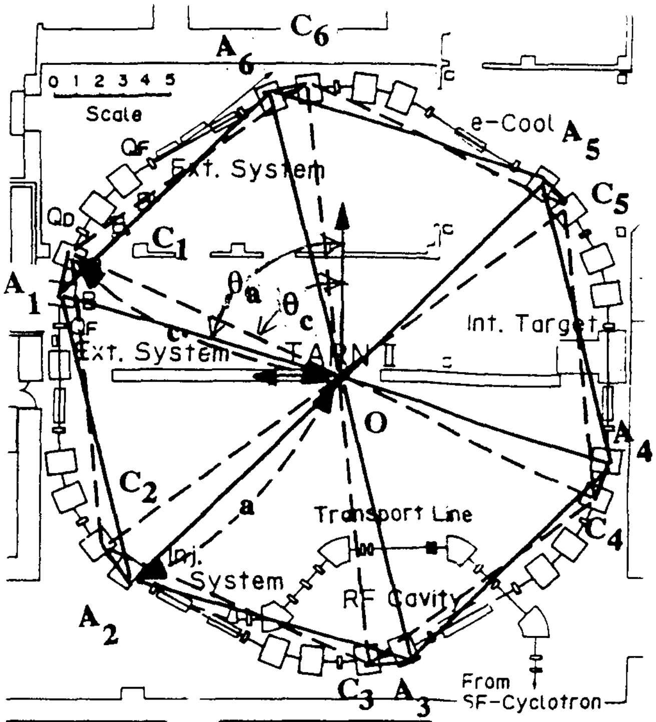

Fig. 3 Constraints to keep the regular hexagonal shape once a subgroup has been well aligned.

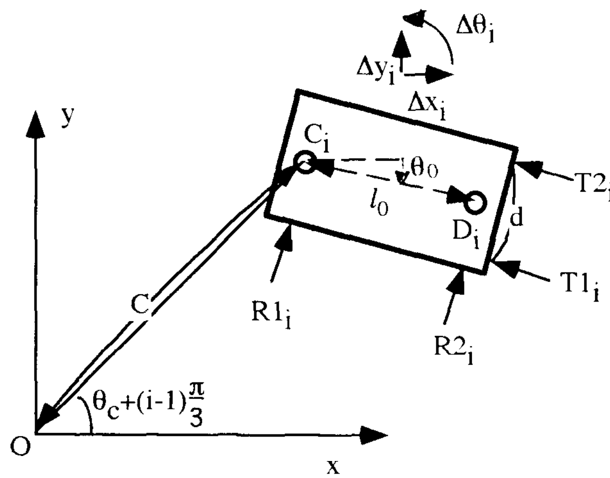

Fig. 4 Definition of the possible position Error of the ith member magnet.

displacements in the horizontal plane and the rotation of the i-th member magnet from the ideal position to be $\Delta x_i, \Delta y_i$ and $\Delta\theta_i$, respectively as is indicated in Fig. 4. If we start the precise alignment after prepositioning, then the displacements and rotation angle, $\Delta x_i, \Delta y_i$ and $\Delta\theta_i$ can well be considered to be small quantities and their higher order terms than second order can be neglected. Thus from the 23 measured distances of $\overline{OC_i}$, $\overline{C_iC_{i+1}}$, $\overline{D_iD_{i+1}}$ (i=1, --,6) and $\overline{OD_i}$ (i=1,--5), the following 23 constraints can be obtained for 18 unknowns of displacements and rotations of the six magnets in the subgroup.

$$\cos\left\{\theta_c + (i-1)\frac{\pi}{3}\right\}\Delta x_i + \sin\left\{\theta_c + (i-1)\frac{\pi}{3}\right\}\Delta y_i = \frac{\overline{OC_i}^2 - c^2}{2c} \quad (i = 1, --, 6) \tag{1}$$

$$\sin\left\{\theta_c + \left(i - \tfrac{1}{2}\right)\frac{\pi}{3}\right\}\left(\Delta x_i - \Delta x_{i+1}\right) - \cos\left\{\theta_c + \left(i - \tfrac{1}{2}\right)\frac{\pi}{3}\right\}\left(\Delta y_i - \Delta y_{i+1}\right) = \frac{\overline{C_iC_{i+1}}^2 - c^2}{2c} \quad (i = 1, --, 6) \tag{2}$$

$$\begin{aligned}&\left[c\cos\left\{\theta_c + (i-1)\frac{\pi}{3}\right\} + l_0\cos\left\{\theta_0 + (i-1)\frac{\pi}{3}\right\}\right]\Delta x_i \\ &+ \left[c\sin\left\{\theta_c + (i-1)\frac{\pi}{3}\right\} + l_0\sin\left\{\theta_0 + (i-1)\frac{\pi}{3}\right\}\right]\Delta y_i + c l_0 \sin\left(\theta_c - \theta_0\right)\Delta\theta_i \\ &= \frac{\overline{OD_i}^2 - c^2 - l_0^2 - 2cl_0\cos\left(\theta_c - \theta_0\right)}{2} \quad (i = 1, --, 5)\end{aligned} \tag{3}$$

$$\begin{aligned}
&\left[c\sin\left\{\theta_c+\left(i-\tfrac{1}{2}\right)\frac{\pi}{3}\right\}+l_0\sin\left\{\theta_0+\left(i-\tfrac{1}{2}\right)\frac{\pi}{3}\right\}\right]\left(\Delta x_i-\Delta x_{i+1}\right)\\
&-\left[c\cos\left\{\theta_c+\left(i-\tfrac{1}{2}\right)\frac{\pi}{3}\right\}+l_0\cos\left\{\theta_0+\left(i-\tfrac{1}{2}\right)\frac{\pi}{3}\right\}\right]\left(\Delta y_i-\Delta y_{i+1}\right)\\
&-l_0\left\{c\cos\left(\theta_c-\theta_0+\frac{\pi}{6}\right)+l_0\cos\frac{\pi}{6}\right\}\Delta\theta_i+l_0\left\{c\cos\left(\theta_c-\theta_0-\frac{\pi}{6}\right)+l_0\cos\frac{\pi}{6}\right\}\Delta\theta_{i+1}\\
&=\frac{\overline{D_iD_{i+1}}^2-c^2-l_0^2-2cl_0\cos\left(\theta_c-\theta_0\right)}{2}\qquad(i=1,--,6)\ ,
\end{aligned}\tag{4}$$

where l_0 is the fixed distance between the two positioning holes in the same dipole magnet (0.850 m) and θ_0 is the angle defined in Fig.4. $\overline{OD_6}$ cannot be measured due to the presence of structure pillar in the wall. If we denote the coefficients of the left-hand sides of these equations to be A_{ij} and the terms of right-hand sides to be b_i, then these equations can be written as

$$A\,\overline{x}=\overline{b}\ ,\tag{5}$$

where $\overline{x}$ denotes 18 dimensional vector composed of $\Delta x_i, \Delta y_i$ and $\Delta\theta_i$ (i=1,---,6) and A and b are the 23x18 matrix and 18 dimensional vector, respectively. In order to obtain the 18 unknovvns. $\Delta x_i, \Delta y_i$ and $\Delta\theta_i$, which simultaneously satisfies 23 independent linear equations (l)~(4), which can be rewritten as Eq. (5), the solution which minimizes the norm, $\|A\,\overline{x}-\overline{b}\|$ is obtained with use of the Scientific Subroutine (SSLII) utilizing Householder's transformation, It is not obvious that this algorithm is valid for the present case, so we have made the check of the validity of this method by generating the random position errors utilizing pseudo-random number. For randomly generated positions of the six member magnets, distances among magnets and the distance of the magnets from the center pole can be calculated. Only using these distance data and using the algorithm above mentioned, the position errors $\overline{x}$ (i.e. $\Delta x_i, \Delta y_i$ and $\Delta\theta_i$ (i=1,---,6)) can be solved, which coincide with the generated ones within 0.002 mm or 0.002 mrad, which is considered quite satisfactory.

For the other subgroups, it is not possible to measure all the distances of the member magnets from the center pole. However, in this case we have added constraints by measuring the distances from the nearby magnets which belong to the already positioned subgroup as indicated in Fig. 3. So in this case, the following relations are added in addition to equations (l)~(4), where c and θ_c are replaced by a and θ_a, respectively although some of them will be missing due to presence of the walls. If we take the subgroup of magnets having positioning holes named A_i and B_i as an example, the relation can be written as

$$\begin{aligned}
&\left[c\cos\left\{\theta_c+(i-1)\frac{\pi}{3}\right\}-a\cos\left\{\theta_a+(i-1)\frac{\pi}{3}\right\}\right]\Delta x_i\\
&+\left[c\sin\left\{\theta_c+(i-1)\frac{\pi}{3}\right\}-a\cos\left\{\theta_a+(i-1)\frac{\pi}{3}\right\}\right]\Delta y_i\\
&=\frac{c^2+a^2-2ca\cos\left(\theta_c-\theta_a\right)-\overline{A_iC_i}^2}{2}\quad(i=1,---,6),
\end{aligned}\tag{6}$$

where θ_a and θ_c are angles defined in Fig. 3. In the present example, $\overline{OA_i}$, $\overline{OB_i}$ (i=2,--,5), A_iA_{i+1}, $\overline{B_iB_{i+1}}$, $\overline{A_iC_i}$(i=1,--,6) are measured and total 26 constraints are imposed on 18 unknowns. In this case, the validity of the algorithm of Eq. (5) with 26x18 matrix A is also checked by generated position errors with use of pseudo-random number and is found that the position error can be solved within 0.002 mm. For other subgroups, similar algorithm is used to align the member magnets.

2.2. Applied Position Feed-Back by the Measured Data

From the solution of simultaneous equation (5), the displacement from the ideal position, Δx_i, Δy_i and $\Delta\theta_i$ are obtained for each magnet. So the position feed back process is decomposed into the positioning of each individual magnet. Real position correction needed for the magnet is calculated as follows

$$\begin{aligned}
R1_i &= -\Delta x_i \cos\left\{\theta_c + (i-1)\frac{\pi}{3}\right\} - \Delta y_i \sin\left\{\theta_c + (i-1)\frac{\pi}{3}\right\} \\
R2_i &= -\Delta x_i \cos\left\{\theta_c + (i-1)\frac{\pi}{3}\right\} - \Delta y_i \sin\left\{\theta_c + (i-1)\frac{\pi}{3}\right\} - l_0 \Delta\theta_i \\
T1_i &= \Delta x_i \sin\left\{\theta_c + (i-1)\frac{\pi}{3}\right\} - \Delta y_i \cos\left\{\theta_c + (i-1)\frac{\pi}{3}\right\} + \frac{d}{2}\Delta\theta_i \\
T2_i &= \Delta x_i \sin\left\{\theta_c + (i-1)\frac{\pi}{3}\right\} - \Delta y_i \cos\left\{\theta_c + (i-1)\frac{\pi}{3}\right\} - \frac{d}{2}\Delta\theta_i \quad ,
\end{aligned} \tag{7}$$

with the notation given in Fig. 4.

By observing the displacement of the magnet in the horizontal plane with use of dial gauges attached to each side of the magnet, the position of the magnet can be well controlled.

3. Real Procedure of the Alignment

In the procedure of the alignment, all the magnets should be set horizontally with use of a water level at first. The precision of the horizontal adjustment is better than 0.2 mrad. Then they are to be set at the same height with the use of the auto level with an optical micrometer. Its minimum scale is 0.1 mm and the precision of the median plane adjustment is better than ±0.1mm including the error due to parallax.

After setting all the magnets in a certain horizontal plane, the algorithm described in the previous section is utilized to make position adjustment for the magnets in that plane. The position feed back is performed based on the distance measurements with use of Invar wire which is stretched with the tension of 8 kg. In Fig. 5, the distometer utilized for the measurement of the distance from the center pole is shown.

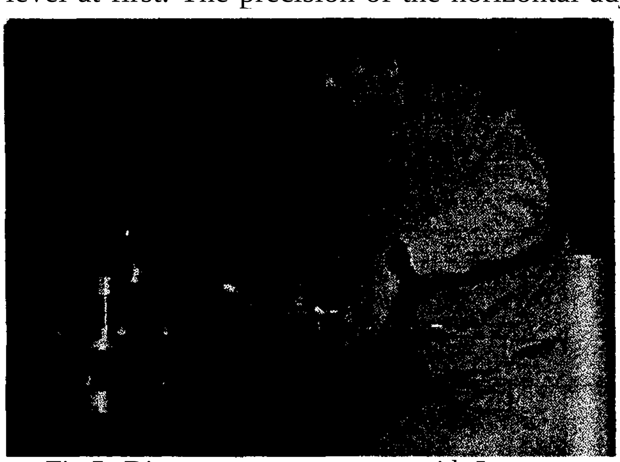

Fig.5 Distance measurement with Invar Distometer.

As the distometer only measures the difference of the distance from the one already known set on a straight rail for the calibration purpose, the absolute value of the distance is calibrated with use of laser linear interferometer (HP5526A). At the present case, the distances between magnets in the same subgroup and the distances of the magnets from the center pole are ~12 m, the length change amounts to the order of 0.06 mm if the temperature change is 5°C even for the case of Invar wire with the expansion coefficient of the order of 10^{-6}. As the experimental hall has no air-conditioning, the distance measurement was performed almost similar time in the day and the absolute length is calibrated at every measurement. In Fig. 6, the length calibration process on the straight rail is shown.

Fig. 6 Absolute Length Calibration with Laser Interferometer.

The precise alignment is started after the pre-positioning with the precision better than ±10mm. With the use of algorithm given in 2.1, the estimated position errors of all the magnets became less than -1 mm after twice iterations. In Fig.7, position deviations of the member magnets after these iterations are shown for the case of alignment of subgroup with alignment holes E_i and F_i as an example. From the results, the convergence of the algorithm seems quite nice.

However, the alignment process stagnated after the position deviations of the magnets became less than 0.5 mm. At first the stiffness of the girder was suspected and the motion of the magnet after position correction was monitored whole night with dial gauges attached to the pillars fixed to the

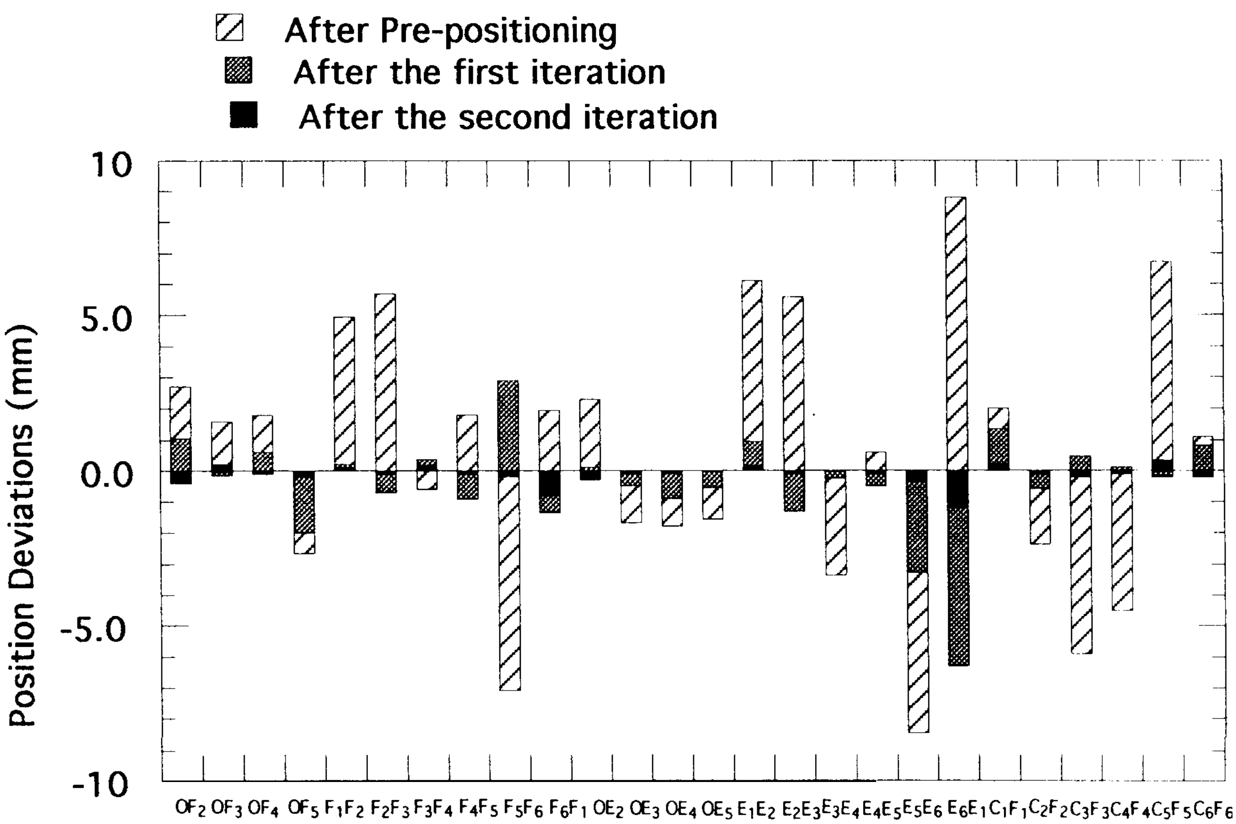

Fig. 7 Position deviations of magnets in subgroup (E,F) after pre-positioning, and the first and second iterations of the position feed back.

floor. However no noticeable movement was found. Finally after making measurements without any position correction, it was found that the floor moved non uniformly day by day with the order of a few hundreds μm as shown in Fig. 8. The global changes are consistent with the thermal expansion coefficient of concrete and we can avoid them by temperature correction. However, the non homologous change as shown in $\overline{OC_3}$ cannot be corrected. So it was decided to terminate the alignment process with the precision of ±0.4 mm. In Table 2, the final deviations of measured

Table 2

Deviations of the finally measured distances from the ideal ones (mm).

i	1	2	3	4	5	6
OA_i	———	0.326	0.128	-0.269	0.177	———
OB_i	———	0.399	0.063	-0.077	0.072	———
OC_i	-0.121	0.043	0.189	-0.111	-0.053	0.043
OD_i	-0.141	0.059	0.116	-0.025	0.104	———
OE_i	———	0.358	0.041	0.041	0.089	———
OF_i	———	0.109	0.104	0.047	-0.196	———
OG_i	———	0.027	0.121	0.087	———	———
OH_i	———	-0.105	0.440	-0.076	———	———
OP_i	———	0.076	0.029	-0.117	0.130	———
OR_i	0.107	-0.122	-0.067	-0.125	-0.175	———
OT_i	———	0.083	0.040	0.012	———	———
A_iA_{i+1}	0.185	0.217	-0.196	0.368	0.003	0.014
B_iB_{i+1}	0.263	0.267	-0.130	0.383	-0.130	0.005
C_iC_{i+1}	0.091	-0.017	0.097	0.076	-0.250	-0.089
D_iD_{i+1}	-0.036	-0.034	0.086	0.155	-0.058	0.047
E_iE_{i+1}	0.224	0.320	-0.001	0.130	0.140	-0.109
F_iF_{i+1}	0.246	0.089	0.047	-0.016	-0.027	-0.037
G_iG_{i+1}	0.085	0.059	-0.097	0.039	0.257	-0.028
H_iH_{i+1}	0.165	0.213	-0.118	-0.052	0.120	-0.043
P_iP_{i+1}	-0.026	-0.067	0.080	0.169	-0.291	———
R_iR_{i+1}	0.131	-0.296	0.160	-0.232	0.229	-0.128
T_iT_{i+1}	———	-0.150	0.008	-0.060	0.268	0.037
A_iC_i	0.067	-0.151	0.157	-0.299	0.067	-0.180
C_iF_i	-0.096	0.067	-0.280	-0.073	0.135	-0.141
C_iH_i	0.097	0.090	-0.312	0.128	0.086	0.060
C_iP_i	-0.005	0.025	0.219	-0.112	0.139	-0.180
C_iQ_i	0.018	-0.009	0.026	-0.089	0.106	-0.242
C_iR_i	-0.138	0.092	-0.189	-0.241	-0.015	0.015
C_iS_i	-0.052	-0.058	-0.158	-0.208	0.027	-0.011
F_iT_i	0.073	-0.038	0.096	0.013	0.028	-0.152
F_iU_i	-0.021	0.041	0.067	0.056	0.065	-0.076

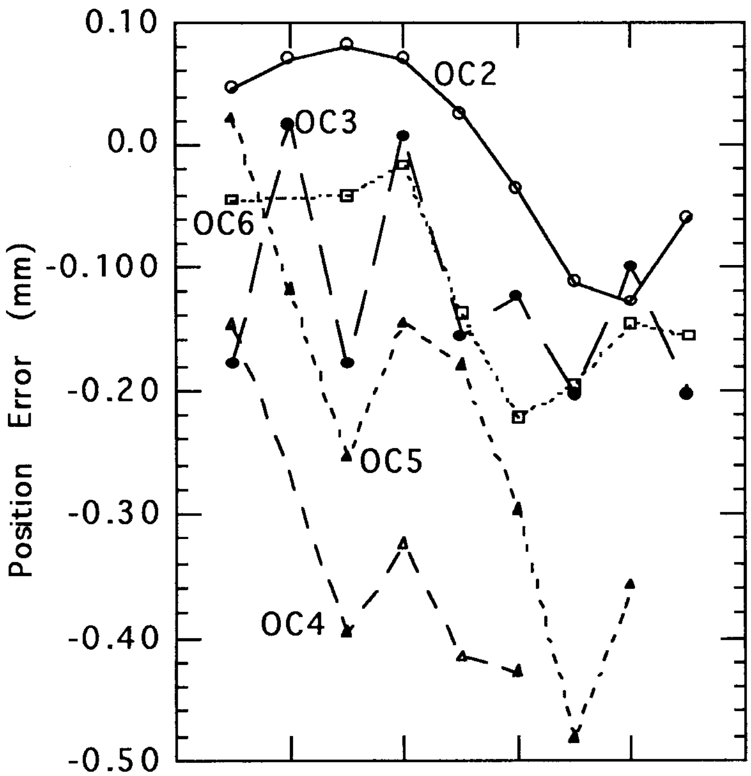

Fig. 8 Daily Variation of distances without Position Correction.

distances from the ideal ones are listed up. In Table 3, the estimated closed orbit distortion is given for the case of position precision of ±0.4 mm together with ±0.1 mm case. From the table, the root mean square sum of the closed orbit distortion seemed to be not so much different and the running in of TARN II was started under this condition, which was very successfully performed [1]. Without any orbit correction, the closed orbit distortion was measured to be a little bit smaller (less than 10mm and 6 mm in horizontal and vertical directions, respectively) than the estimation given in Table 3, which was corrected with use of the electrostatic position pick-ups with high sensitivity and correction coils wound on the dipole magnets or vertical steering magnets[3] and the closed orbit distortion is reduced less than 1 mm as shown in Fig. 9[4]. Thus the present method of the alignment seems to have worked well although some difficulty existed to keep the precision of ±0.1mm originally aimed at due to the non uniform movement of the floor, because the experimental hall was made of three different parts made at the different times and on the different bases.

Acknowledgements

The authors would like to present their sincere thanks to Prof. Y. Hirao for his continuous encouragement during the work. They are very grateful to Prof. K. Endo at KEK for his fruitful discussion about alignment of magnets for synchrotron ring and also his aids to lend us the Invar distometer during the present alignment process. Their thanks are also due to other members of accelerator division of INS who collaborated on TARN II. Cooperation of Nihon Kensetsu Kogyo is also greatly appreciated.

REFERENCES

[1] T. Katayama, “Cooler Synchrotron TARN II, Present and Future”, Proceedings of the 19th INS Symposium, COOLER RINGS AND THEIR APPLICATIONS, Tokyo, Japan (1990) pp21-30.
[2] K. Endo and M. Kihara, “Precise Alignment of Magnets around Accelerator Ring”, KEK Report, KEK-74-3 (1974).
[3] T. Tanabe et al., “Vertical COD Correction”, Institute for Nuclear Study, University of Tokyo, Annual Report 1992, p120.
[4] T. Watanabe et al., “Beam Position Monitoring System and C.O.D. Correction at the Cooler Synchrotron TARN II”, to be submitted to Nuclear Instrument and Methods.

Table 3

Closed Orbit Distortion

Horizontal Direction				Vertical Direction			
Source	Tolerance	C.O.D.(mm) In Dipole	C.O.D.(mm) in Q	Source	Tolerance	C.O.D.(mm) In Dipole	C.O.D.(mm) in Q
Field Error	$5x10^{-4}$	10.09	11.11	Tilt of Dipole	$2x10^{-4}$	5.49	5.73
Length Error	$5x10^{-4}$	10.09	11.11				
Stray Field at Injection	0.25 G	4.09	4.50	Stray Field at Injection	0.10G	2.22	2.22
Displacement of Q	0.1 mm (0.4 mm)	1.06 (4.24)	1.17 (4.68)	Displacement of Q	0.1 mm	1.44	1.55
r.m.s. sum		14.88 (15.44)	16.39 (17.00)	r.m.s. sum		6.09	6.36

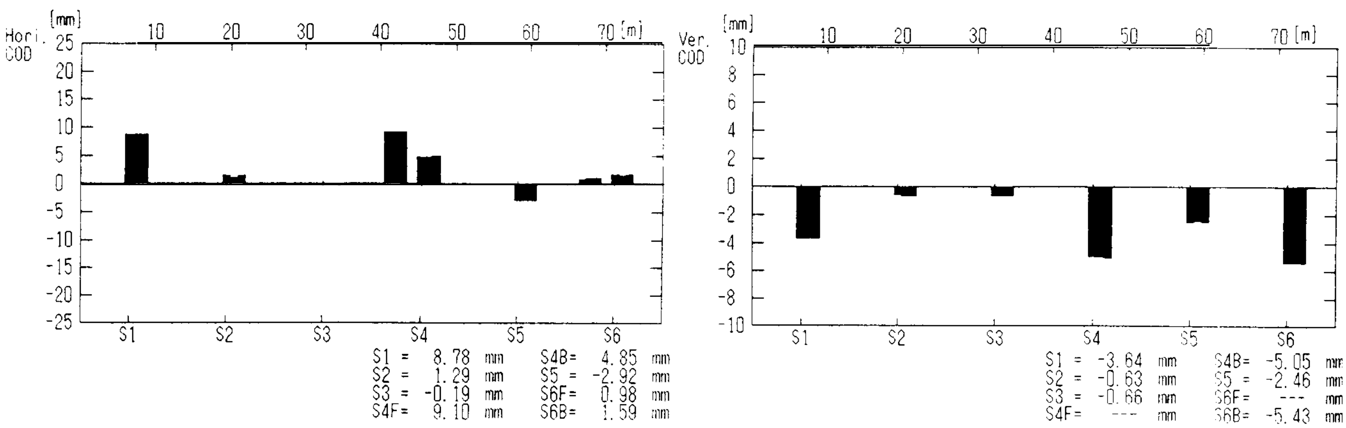

Horizontal Direction　　　　Vertical Direction

Fig. 9 (a) Closed Orbit Distortion without Orbit Correction.

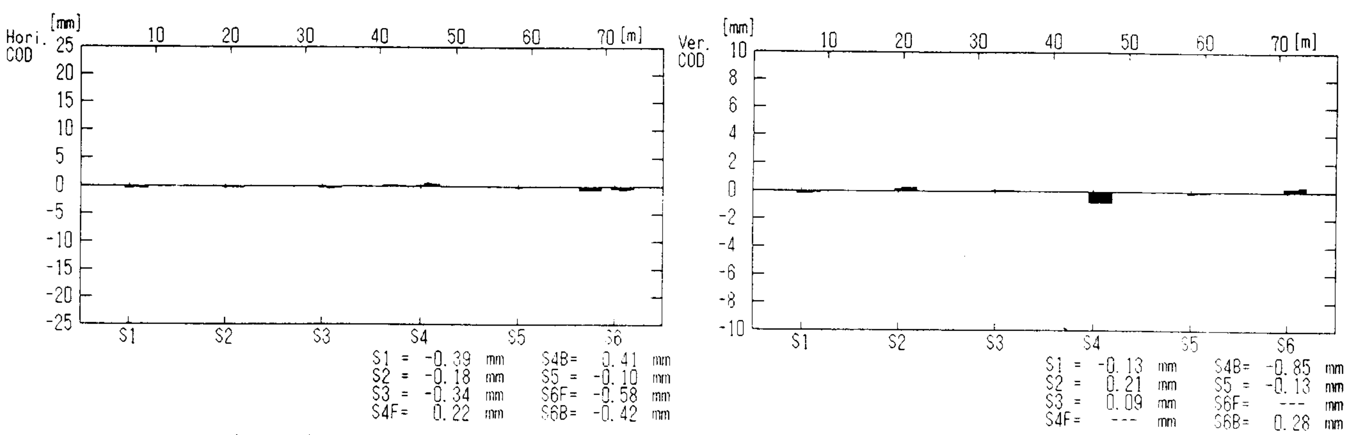

Horizontal Direction　　　　Vertical Direction

Fig. 9 (b) Closed Orbit Distortion with Orbit Correction.